STATUS OF STUDIES OF PULSED HEAT LOAD INFLUENCE ON TUNGSTEN AT BETA FACILITY AND STATIONOF SR SCATTERING "PLASMA" IN BINP

A.S. ARAKCHEEV, V.M. AULCHENKO, I.I. BALASH, A.V. BURDAKOV,
A.D. CHERNYAKIN, V.A. DOKUTOVICH, O.V. EVDOKOV, I.V. KANDAUROV,
A.A. KASATOV, S.R. KAZANTSEV, A.V. KOSOV, V.V. KURKUCHEKOV, V.A. POPOV,
M.R. SHARAFUTDINOV, L.I. SHEKHTMAN, B.P. TOLOCHKO, YU.A. TRUNEV,
A.A. VASILYEV, L.A. VAIGEL, L.N. VYACHESLAVOV, V.V. ZHULANOV
Budker Institute of Nuclear Physics SB RAS
Novosibirsk, Russia
Email: A.S.Arakcheev@inp.nsk.su

Abstract

Experiments simulating the pulsed heat loads expected in the ITER divertor were carried out at the BETA facility in the Budker Institute. A distinctive feature of BETA is the ability to study the processes of erosion of tungsten in situ during the heating and immediately after it in the cooling stage. The image of the target surface in its own thermal radiation shows that even under a homogeneous electron beam, having a Gaussian profile with a full width at a half maximum of about 17 mm, hot spots are visible with a temperature much higher than the temperature of the surrounding area. Analysis with SEM and microsections shows that overheating is associated with a decrease in heat removal from these surface areas due to cracks caused by pulsed heating. The method of laser illumination reveals a two-stage process of erosion of the polished tungsten surface after the first heat load. Initially, the surface roughness begins to increase and then decreases within a few milliseconds upon cooling to a value 2-3 times higher than the initial level of roughness. The second stage of surface modification, corresponding to surface cracking, occurs spontaneously and rapidly develops for a time of the order of ten microseconds on a sample already cooled to room temperature. The delay in the initiation of cracking of the surface exceeded the time required for the transition from the plastic to the brittle state by 3-4 orders of magnitude.

Synchrotron radiation scattering station "Plasma" develops diagnostics of deformations and stresses in the material under the pulse heat load using the diffraction dynamics. This diagnostic has three principal features: measurements with time resolution, measurements inside the material and measurements with the depth resolution. Currently, the measurement of the dynamics of the shape of the diffraction peak is shown

1. INTRODUCTION

The BETA facility (Beam of Electrons for material Test Applications) was developed on the basis of an intense pulsed electron beam source in the Institute of Nuclear Physics in Novosibirsk [1]. The facility is designed for the experimental simulation of pulsed heat loads with the power density and duration similar to the parameters expected in the ITER divertor. An important difference of BETA from many other facilities, also designed for experimental simulation of the pulsed heat loads on materials, is the ability of measuring the modification of materials during the heating and immediately after it. Optical diagnostics made it possible to measure the uneven temperature distribution over the surface of the sample during its heating and subsequent cooling, while the surface was heated uniformly. The reasons and consequences of the formation of the overheated areas are discussed in the paper. Another optical diagnostic used at BETA facility was the based on the measurements of the continuous laser radiation scattered on the exposed surface.

In addition to optical diagnostics for dynamic measurement of the effect of pulsed heating of materials, the diagnostics based on scattering of synchrotron radiation is currently being developed at the synchrotron radiation scattering station "Plasma" [2]. This diagnostic has three principal features: measurements with time resolution, measurements inside the material and measurements with the depth resolution. The first results of the measurements of the diffraction dynamics are obtained.

2. BETA FACILITY

The BETA test facility uses an electron beam (30-110 keV, up to 80 A), which is generated in the source with an arc plasma emitter and a multi-aperture diode electronic optical system. The pulse of the beam power has an almost rectangular shape with a duration of 100-300 μs [1,3] and is used to heat a tungsten target. A schematic image of the facility is shown in Fig. 1. The electron beam is transported in the guiding magnetic field, which increases from 0.006 T in the source region to 0.07 T-0.2 T on the target. When passing through a convergent magnetic field, the beam adiabatically contracts and hits the tungsten target 1.6 m away from the accelerating

diode. The compressed beam provides thermal loads up to 15 GWm^{-2} on an area of about 1 cm^2. In typical operating modes, the beam current density increases by a factor of 30 with an efficiency of more than 90%. The compressed beam transfers about 60% of its energy to the tungsten target, as follows from direct calorimetric measurements [3]. The interaction of the electron beam with the target affects the operation of the accelerating diode, therefore at maximum power the beam duration is usually less than 200 μs, and at moderate power the duration reaches more than 300 μs. The volume of the experimental chamber, separated by a gate valve from the vacuum vessel of the beam source, is equipped with two diagnostic inserts with four diagnostic ports each. The diagnostic set 1 is located in the target plane and is intended for parallel viewing of the ablative plume and dust particles near the target. A dust measuring system based on small-angle light scattering, as well as visualization of dust particles by their thermal radiation using fast CCD and ICCD cameras were used here. As a rule, we use 1.4-megapixel CCD cameras with a minimum exposure time of 7 μs and 0.8 megapixels of ICCD with a minimum exposure of 2 μs. The diagnostic set 2 is located 41 cm from the target closer to the electron beam source and is used for frontal observation of the target surface. Here we use fast visualization of the target surface in the near infrared spectral range and in the light of a 535 nm CW laser. The suppression of the target thermal radiation using laser illumination is provided by narrow-band (0.2 nm and 1 nm) spectral filters centered at the wavelength of the laser.

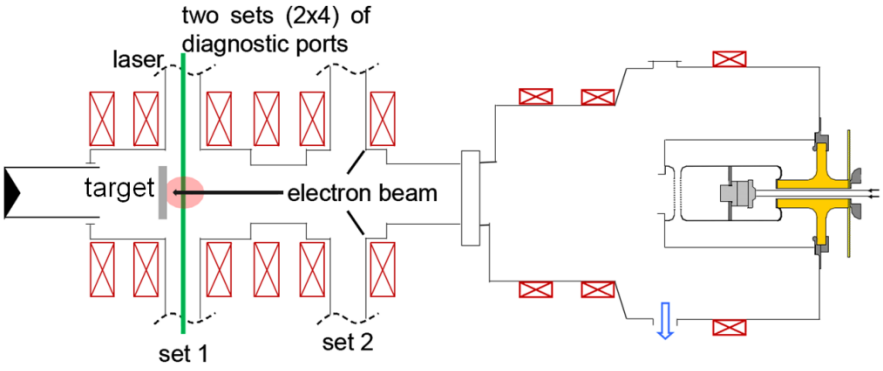

FIG. 1. The schematic layout of BETA facility.

3. IMAGING OF THERMAL RADIATION

Front view of the tungsten plate is captured by a fast CCD camera with 1.4 MP resolution supplied with an infrared filter. The final spectral sensitivity of the system enables to obtain a picture of thermal radiation in near infrared range (880 – 1020 nm) without interference from the light of ablation plume. Optical magnification is 1/2.7. It determines spatial resolution of the images, which is about 20 μm. 2D distribution of the surface temperature is reconstructed using absolute calibration with tungsten ribbon lamp.

Samples of rolled tungsten with thickness 3-4 mm were used in following experiments on high heat loads. IR-imaging revealed formation non-uniformity in thermal radiation of the surface. Average energy load of 0.8 MJ/m2 near melting threshold caused cracking of the tungsten sample. Crack edges were clearly detected during electron beam impact because of their increased thermal radiation (Fig. 2). It was found that slight crack net forms after first heat load. It becomes denser and more distinguishable with subsequent exposures. Propagation of this structure becomes slower after fourth pulse.

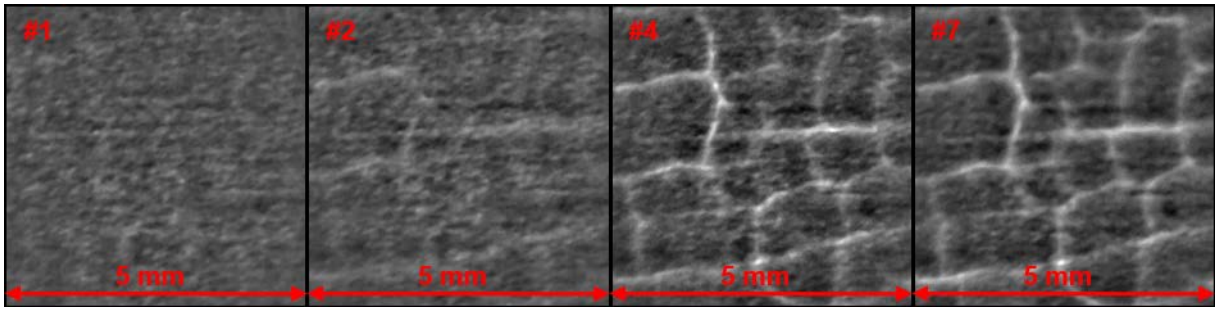

FIG. 2. Images of the central area of the target soon after heat load. Dome-like background light profile was subtracted for emphasizing of thermal radiation inhomogeneities.

The target irradiation leads to its surface erosion. The initially damaged tungsten target with crack network was imaged after beam impact with average energy load ~1 MJ/m^2 and F_{hf}~ 70 MJm^{-2}s$^{-0.5}$. 2D temperature distribution was obtained from IR-image 20 μs after heat end (Fig. 3(a)). It shows material melting on the crack edges in the center of the target. Subsequent SEM survey showed intense melting of the surface layer near these areas (Fig. 3(b)). Following transverse microsection of the target revealed propagation of the cracks along the surface at a depth 0.1 – 0.2 mm (Fig. 3(c)). Such cracks start from perpendicular ruptures and develop into the material bulk. This target damage is responsible for suppression of the heat transport from the surface and can lead to appearance of the areas with excessive temperature and detached parts of the sample.

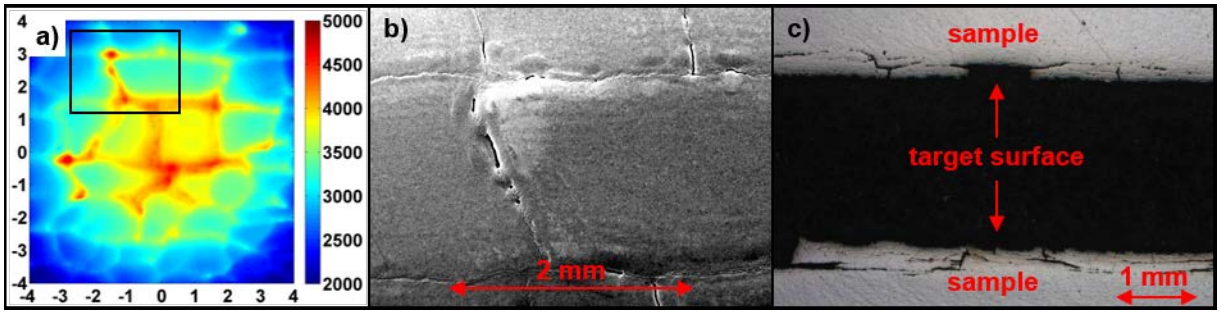

FIG. 3. a) Temperature distribution on the surface after 20 μs after beam impact; b) SEM image of the area marked with black rectangular on (a); c) transverse microsection of the sample.

Investigation of the target surface after impact of more than 100 exposures with heat loads of ~1 MJ/m^2 and F_{hf}~90 MJm^{-2}s$^{-0.5}$ showed existence of the local hot areas. These overheated regions remained on the sample after more than 5 ms after beam termination. Temperature excess over surrounding space was about 500K. Following SEM survey exposed severe detachment of the tungsten layers from the bulk of the material.

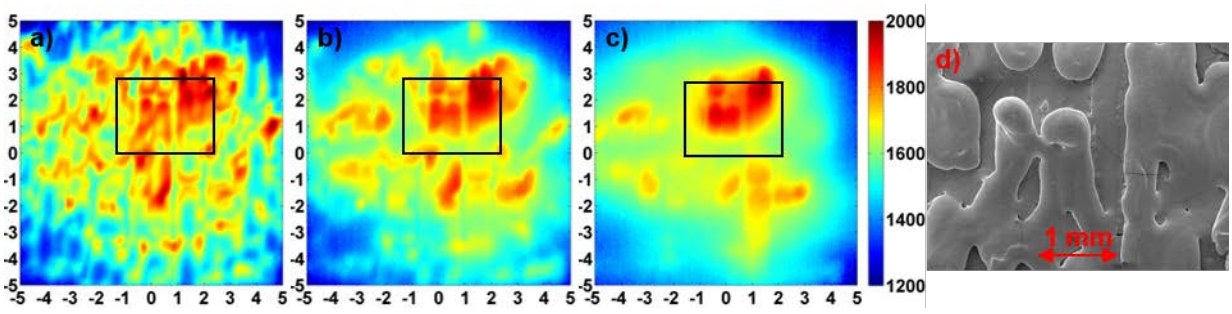

FIG. 4. Temperature distribution after electron beam termination in different times: a) 350μs, b) 1850 μs, c) 7850 μs. d) SEM picture of the area marked with black rectangular on previous images.

4. OBSERVATION OF SCATTERED LASER RADIATION

In these experiments, we use tungsten with a grain orientation parallel to the surface. Samples having size 25x25x3 mm^3, which surface 25x25 mm^2 was polished using abrasive processing in the optical workshop at the Budker Institute. After completion the polishing, the targets were ultrasonically cleaned with successive use of water with detergent, distilled water and acetone. The target was placed in the experimental chamber at room temperature and subjected to a single irradiation pulse with the following characteristics: a circular region of action with a Gaussian heating profile at FWHM = 17 mm, and F_{HF}=30 MJ m^{-2} $s^{-0.5}$ at the maximum. The duration of the electron beam was set to 250 μs, and the electron energy was set equal to 70 keV in these experiments The optical layout for measuring the intensity of scattering of laser radiation is shown in Fig. 1 and 5. The light of a continuous laser at 532 nm is directed to the target by means of a mirror M1 located inside the vacuum chamber near the vertical port of the set 2, as shown in Fig. 1 and 5. The laser beam has an elliptical shape with dimensions 9x6 mm^2 on the surface of the target and reflected from it specularly. The optical system is aligned in such a way that the laser beam reflected by the target surface specularly, is directed through the center of the lens 1 and along the optical axis of the detection system. The detection system is used in the dark field mode [4], when the specular laser beam is blocked on the surface of the lens 1 by the beam absorber BA, and only light scattered by the target surface and other optical elements can reach optical detectors.

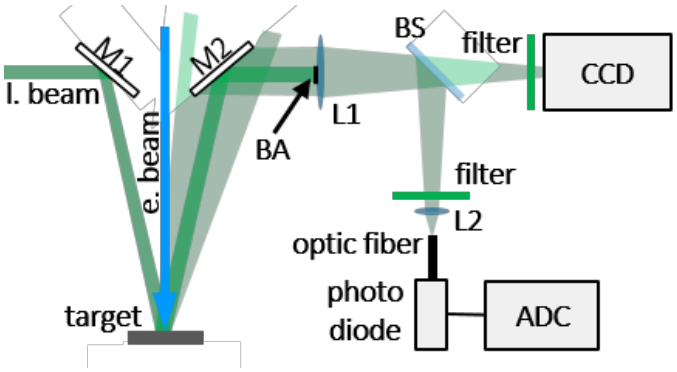

FIG. 5. The layout of recording of laser light intensity scattered by the tungsten target. Here l.beam is the probe 532-nm laser beam, M1 and M2 are mirrors; BA is a beam absorber; BS is a beam splitter.

The scattered light is recorded using two detection systems separated by a beam splitter BS [5]. The first system takes an image of the target surface with a fast CCD camera. The second system continuously records the intensity of the laser radiation, scattered by the target into the angular aperture of the optical system, using a photodiode and an ADC. The angular aperture is determined mainly by mirror M1, which selects a fraction of diffuse halo around the specular laser beam. This halo is created by diffuse scattering on imperfections of the target surface created by the thermal shock. The first system is similar to the laser backlight measurement technique described earlier in [6, 7], but now it is used in the dark-field imaging mode. The second detection system is new and its data allow one to see an interesting time dependence of the intensity of the scattered light, shown in Figure 6. The waveform corresponds to the behavior of the new polished tungsten surface during and after the thermal shock. An overview of the time dependence of the intensity of scattered radiation in Fig. 6a shows two sharp increases, separated by an interval of 400 ms. After the first rise, a noticeable decrease in intensity is observed until reaching a stationary level, and after the second rise, the level of scattered light remains constant. A detailed review of the first rise in Fig. 6b shows that the light intensity increases almost linearly during the 250 μs, duration of the heating pulse marked with dashed lines, and then gradually decreases to a new stationary level within a few milliseconds. The second increase in intensity occurs spontaneously and much faster, the time for the entire growth process to reach a stationary level in this case is only 30 μs. The detailed shape of this rise is shown in Fig. 6c where the sampling points separated by 5 μs are marked by squares.

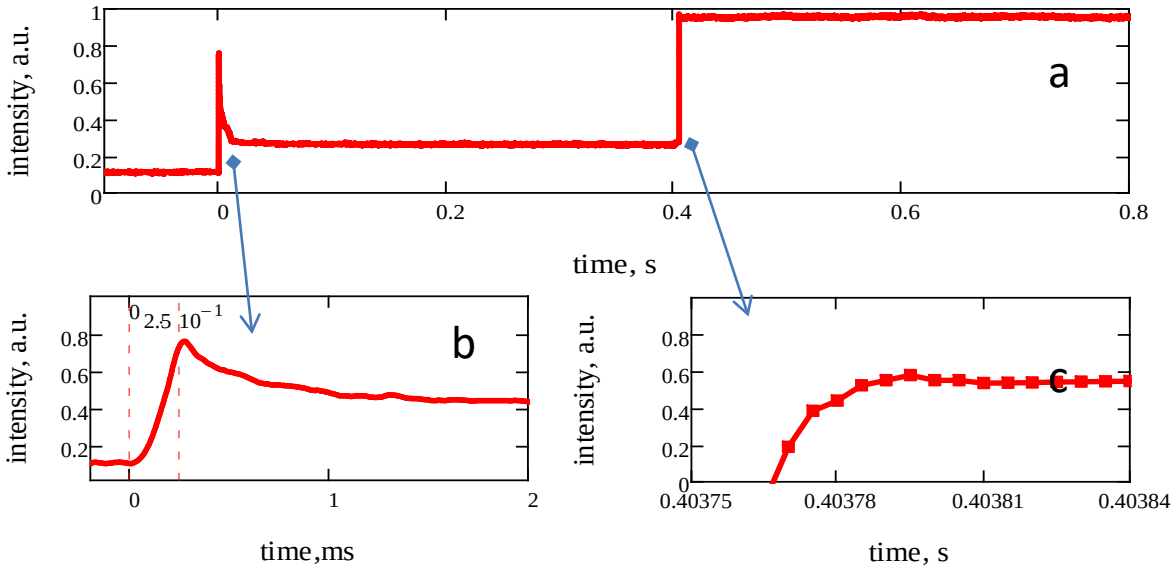

FIG. 6. Waveforms of the intensity of laser radiation scattered by the surface of a tungsten target. The entry level signal is determined by the imperfections of the new polished sample surface and the subsequent optics of the detection system. The process of erosion of the surface begins at the instant t = 0, when a single thermal shock occurs with a duration of 250 μs. Its beginning and end are marked by dotted lines in Figure 4b.The second increase in the intensity of the scattered light begins spontaneously at about 0.4 sec and corresponds to rapid cracking in an area of 9x6 mm², illuminated by a probing laser beam, near the center of the heated region.

The first peak of the intensity of the scattered light can be interpreted as the effect of the development of the roughness mechanism, schematically considered in [8]. A few microseconds after the start of heating, the temperature of the surface layer about 5 μm thick, associated with the mean free path of electrons with an energy of 70 keV, reaches 500° C, which corresponds to the brittle-to-ductile transition. After this, the thermal expansion of the heated surface layer occurs unevenly, having a scale irregularities of the order of the grain size or even more. The height of this inhomogeneous thermal expansion and the surface roughness associated with it increase with increasing temperature and thickness of the heated layer. The recorded signal is associated with the scattering of light on the roughness formed on the surface. After the heating ceases, the cooling stage of the surface begins, during which the roughness decreases due to the reverse plastic deformation [9], which leads to a substantial decrease in the scattering signal. However, having reached a return to the fragile state, the change in the roughness height and the scattering signal rapidly slows down and remains unchanged until the next increase in the intensity and scattering. It should be noted that the time delay between the two rises of the scattering signal varies widely from sample to sample.

A strong second rise in the intensity of scattered light is determined by growth of the ridges during the cracking process. Residual tensile stresses along the surface cause elastic compression in the direction perpendicular to the surface (Poisson effect) [9]. The formation of a crack perpendicular to the surface leads to the release of stress in the region near the crack. Thus, the removal of tension leads to a local disappearance of the mentioned deformation and, consequently, to an elevation of the surface around the crack. The height of the ridge thus formed is much less than the depth of the crack, since the relative deformation of tungsten is much less than unity. However, the width of the ridge should be approximately equal to the depth of the crack, since the size of the region of stress decrease depends on the depth of the crack. Preliminary analysis shows that in our experiments the network of ridges is in good agreement with the network of cracks recorded on the same sample using SEM. Raising the edges in the cracks, which should also lead to the formation of a network of ridges, can be also noticed in the results of experiments of other groups [10]. Attention is drawn to the variety of time scales of processes of surface damage by a thermal shock. The increase in roughness first proceeds simultaneously with heating, although the time for the reduction of the roughness upon cooling the surface exceeds the time of its increase by more than an order of magnitude. Especially unexpected was the temporary delay in the onset of cracking, which was three orders of magnitude greater than the time required to reach the transition temperature into the brittle regime, and exceeded the duration of the cracking process by four orders of magnitude. The estimated temperature of the heated surface during cracking is about room temperature. The observed dynamics of cracks requires further study.

5. SCATTERING STATION “PLASMA”

The effect of pulsed heating of materials, the diagnostics based on scattering of synchrotron radiation is currently being developed at the "Plasma" station [2]. This diagnostic has three principal features: measurements with time resolution, measurements inside the material and measurements with the depth resolution. This diagnostic uses the Laue diffraction on a tungsten single crystal with a thickness of up to 500 μm. The heat load is simulated by a YAG laser with energy of up to 50 J and a duration of about 140 microseconds. The heat load leads to deformation of the crystalline plane on which diffraction occurs. Because of this, the position and shape of the diffraction peak change. The shape and position of the diffraction peak is measured by the DIMEX detector [11]. The detector makes 100 frames with duration of 20 microseconds. It is planned to calculate the dynamics of the distribution of deformations in the material using the measurement of the shape of the peak. Currently, the measurement of the dynamics of the shape of the diffraction peak is shown

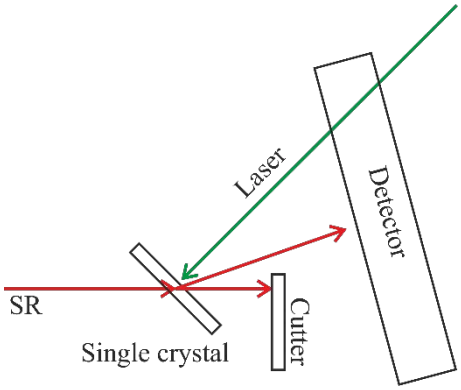

FIG. 7. Scheme of experiment at scattering station “Plasma”.

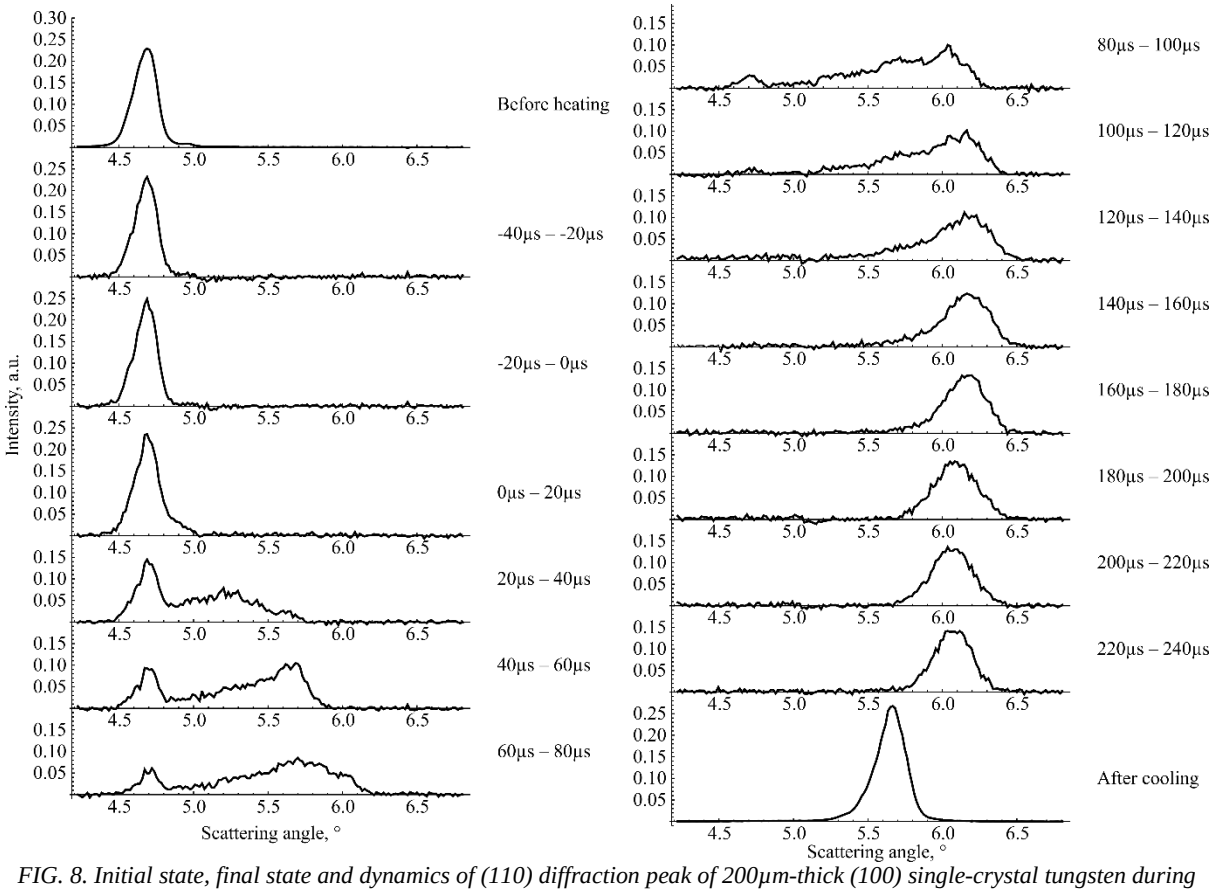

FIG. 8. Initial state, final state and dynamics of (110) diffraction peak of 200μm-thick (100) single-crystal tungsten during pulsed heat load. The heating started approximately at 0μs and finished at 140μs.

The experiments were carried out at the scattering station “Plasma” on the 8th beamline of the synchrotron radiation source of VEPP-4. The scheme of experiment is presented in Fig. 7. The experiments were performed with the polychromatic synchrotron radiation from the wiggler [12]. Synchrotron radiation with an energy close to the K-edge of tungsten (69:525keV) was to minimize the attenuation in the material. The cross-section of the initial beam of synchrotron radiation was 1mm ×1mm. The most intensive diffraction peak (110) was measured. The scattering angle 2θ corresponding to the energy and diffraction peak is about 4.5°. The (100) mosaic single crystal tungsten was chosen for the experiments in order to provide presence of plane (110) inclined at 45° to the surface and absence of preferential direction for plastic deformation along the surface. We used the one-dimensional detector DIMEX to measure the dynamics of the diffraction peak shape. The distance from the sample to the detector was about 300mm. The detector yielded 100 frames containing signals of 512 channels. The width of each channel is 100μm.

By the presented layout of experiment, we measured the dynamics of the (110) diffraction peak of 200μm-thick (100) single-crystal tungsten. Fig. 8 presents the dynamics, as well as the initial and final states, of the peak. The three stages of the diffraction peak evolution can be clearly distinguished here: heating of the surface, equalizing of the temperature distribution transversely to surface, and cooling to the room temperature.

At the first stage, approximately from 0μs and till 140μs (heating by a laser pulse,) the surface temperature increases. The scattering angle of X-ray grows with the temperature. Consequently, the right side of the diffraction peak moves to the right. The temperature of the back side of the sample stays close to the initial one during the stage. It means that layers with all temperatures from the initial one to the instantaneous maximum one are presented in the temperature distribution. So, the signal of the scattered radiation covers the whole range from the initial position to the moving right side of the diffraction peak. The equalizing of the temperature distribution transversely to the surface occurs at the second stage (approximately from 140μs to 240μs). The evolution of the diffraction peak shape significantly slows down after the second stage because the further temperature distribution change is caused by heat removal along the sample surface. The heat removal along the surface is much slower than the equalizing of the temperature distribution transversely to the surface. So, there are no recognizable changes in the diffraction peak shape in the subsequent 14 frames, which are not shown in Fig. 8. The lasting evolution of diffraction peak shape during the third stage (cooling to the room temperature) was not measured. However the final state of the diffraction peak shape was measured several seconds later. Note that the initial and final states are statical. So, the diffractograms were measured much more accurately. According to the relation between the temperature and scattering angle, the latter decreases after cooling.

6. SUMMARY

Crack net formation and development was observed with serial heat loads. Melting of the crack edges was found with imaging with laser light illumination and 2D temperature distribution. Propagation of the crack along the surface was revealed with cross-section cutting. Detached parts of the target with excessive temperature of ~500 K over surrounding sample were found after more than 100 shots.

The illumination of the target surface with the laser light during and after the heating pulse made it possible to trace the development of the processes of growing the roughness and the formation of a network of cracks in time. The first experiments revealed unexpectedly large delays in cracking from thermal shock and a very rapid cracking process occurring almost simultaneously on the entire heating area. This requires further study, both experimentally and theoretically.

The measurements of the dynamics of the diffraction peak shape during pulsed heat load were carried out at the scattering station “Plasma” on the 8th beamline of the synchrotron radiation source of VEPP-4. The changes in the diffraction peak shape were clearly seen. The changes qualitatively agree with the theoretical predictions, and the value of change in the scattering angle agrees with the estimation. The three stages of the diffraction peak evolution can be clearly distinguished: heating, equalizing of the temperature, and cooling. The observed change in the diffraction peak shape confirms that the mechanism of the changes is rotation of crystal plane rather than bending of material. Moreover, the constancy of the initial diffraction peak position means that the bending is negligible.

ACKNOWLEDGEMENTS

The experiments at BETA facility were supported by Russian Science Foundation (project 17-79-20203). The experiments at station of synchrotron radiation scattering "Plasma" were supported by Russian Science Foundation (project 14-50-00080).

REFERENCES

[1] VYACHESLAVOV L.N., ARAKCHEEV A.S., BURDAKOV A.V. et al. Novel electron beam based test facility for observation of dynamics of tungsten erosion under intense ELM-like heat loads, AIP Conf. Proc. 1771 (2016), 060004.

[2] ARAKCHEEV A.S., ANCHAROV A.I., AULCHENKO V.M. et al. Status of Dynamic Diagnostics of Plasma Material Interaction Based on Synchrotron Radiation Scattering at the VEPP-4 Beamline 8, Physics Procedia, 84 (2016), 184.

[3] TRUNEV YU.A., ARAKCHEEV A.S., BURDAKOV A.V. et al. Heating of Tungsten Target by Intense Pulse Electron Beam, AIP Conf. Proc. 1771 (2016), 060016.

[4] HOBBS P.C.D. Building Electro-Optical Systems. Making It all Work 2ed., Wiley (2009).

[5] VASILYEV A.A., ARAKCHEEV A.S., BATAEV I.A. et al. Observation of the tungsten surface damage under ITER-relevant transient heat loads, AIP Conf. Proc. 1771 (2016), 060013.

[6] VYACHESLAVOV L.N., ARAKCHEEV A.S., BATAEV I.A. et al. Diagnostics of the dynamics of material damage by thermal shocks with the intensity possible in the ITER divertor, Physica Scripta 93 3 (2018), 035602

[7] VASILYEV A.A., ARAKCHEEV A.S., BATAEV I.A. et al. In-situ imaging of tungsten surface modification under ITER-like transient heat loads, Nucl. Matter Energy 12 (2018), 553-558.

[8] LINKE J., LOEWENHOFF T., MASSAUT V. et al. Performance of different tungsten grades under transient thermal loads, Nucl. Fusion 51 (2011), 073017.

[9] ARAKCHEEV A.S., SKOVORODIN D.I., BURDAKOV A.V. et al Calculation of cracking under pulsed heat loads in tungsten manufactured according to ITER specifications, J. Nucl. Mater. 467 (2015), 165.

[10] WIRTZ M., LINKE J., PINTSUK G. et al. Comparison of thermal shock damages induced by different simulation methods on tungsten, J. Nucl. Mater. 438 (2013), S833–S836.

[11] AULCHENKO V.M., EVDOKOV O.V., SHEKHTMAN L.I. et al. Detector for imaging of explosions: present status and future prospects with higher energy x-rays, JINST, 3 (2008), P05005.

[12] VOBLY P., BARANOV G., LEVICHEV E. et al. Design and Magnetic Measurements of a Hybrid Wiggler for SR Research Program at VEPP-4. IEEE Transactions on Applied Superconductivity 28 3 (2018), 4101403.